

OFDM SPECTRUM SCULPTING WITH ACTIVE INTERFERENCE CANCELLATION: KEEPING SPECTRAL SPURS AT BAY

Jorge F. Schmidt and Roberto López-Valcarce

Department of Signal Theory and Communications
University of Vigo, 36310 Vigo, Spain
email: {jschmidt, valcarce}@gts.uvigo.es

ABSTRACT

Active interference cancellation (AIC) is an effective technique to shape the OFDM spectrum, providing deep notches over protected bands without affecting receiver design. However, AIC typically introduces spectrum overshoot, of concern if compliance with a spectral emission mask is required. Most AIC designs neglect these spectral spurs, focusing on minimization of out-of-band radiation. We present a novel design that explicitly takes spectral spurs into account. The resulting optimization problem is convex and can be efficiently solved, although for systems with a large number of subcarriers the computational effort can be significant. A suboptimal solution based on a previous AIC design with a maximum power constraint is also proposed. Its performance is close to optimal while obtained at a much lower computational cost, comparing favorably to previous schemes.

Index Terms—Active Interference Cancellation, Spectrum Sculpting, Cognitive OFDM.

1. INTRODUCTION

Orthogonal Frequency Division Multiplexing (OFDM) has been widely adopted as the modulation technique for many broadband wireless communication systems. It is particularly well suited to cognitive systems, as the transmit signal can be easily adjusted to the available spectrum by turning on or off different sets of subcarriers [1, 2]. In this way, spectrum holes are generated to avoid interfering to primary users lying within the OFDM band. Unfortunately, merely turning off subcarriers in order to minimize Out-of-Band Radiation (OBR) is inefficient: due to the high sidelobe levels of the Fast Fourier Transform (FFT) employed in OFDM, a large number of subcarriers adjacent to the protected band must be turned off to achieve sufficient OBR reduction.

More efficient approaches to OBR reduction do exist. In particular, Active Interference Cancellation (AIC) techniques

have gained interest recently [3]–[12]: they yield good performance and, in contrast with precoding-based approaches [13]–[21], they do not require the transmission of side information or implementing specific decoding operations at the receiver side, thus allowing straightforward integration in current OFDM systems. AIC reserves a (small) subset of subcarriers (termed *cancellation subcarriers*, or simply *cancellers*) for OBR reduction, without altering the remaining *data subcarriers*. This operation is transparent to the receiver, which just discards cancellation subcarriers prior to data decoding.

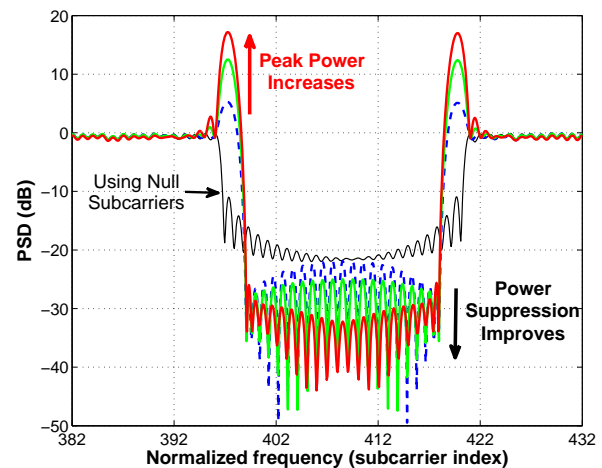


Fig. 1. Power spectra of OFDM signals after AIC, showing typical spectral spurs.

A typical, often overlooked AIC byproduct is PSD overshoot, illustrated in Fig. 1. As the fraction of the total available power given to the cancellers is increased, the reduction in OBR improves but, on the other hand, the spectral peaks or “spurs” located at the positions of the cancellers become substantially larger. These spurs can be a limiting factor for the application of AIC-based OBR reduction methods when compliance to a tight spectral emission mask is required.

The problem of keeping spurs under control was considered in [7, 10]. As spurs appear at the positions of cancellers,

Work supported by the Spanish Government, ERDF funds (TEC2010-21245-C02-02/TCM DYNACS, CONSOLIDER-INGENIO 2010 CSD2008-00010 COMONSENS) and the Galician Regional Government (CN 2012/260 AtlantTIC).

the usual total power constraint is replaced in [7] with multiple constraints, one for each canceller. However, since the constraints are placed directly on the magnitude of the cancellers' coefficients, their impact on the PSD is not immediately clear, and some case-specific trial and error becomes necessary in order to set the constraint values for satisfactory results, with no guarantee of optimality regarding OBR as the criterion of interest. On the other hand, the approach in [10] addresses spectrum overshoot by thresholding the singular values of certain matrix featuring in the unconstrained solution. Although this seems an effective means to reduce spurs at low computational cost, it is an ad hoc method, so that, similarly to [7], the performance obtained in terms of OBR reduction is not clear; in addition, its flexibility is rather limited, particularly if the number of cancellers is small.

In contrast, we present a novel AIC design which, similarly to [12], is directly based on the OBR cost, but imposing a single constraint on the maximum peak value of the resulting PSD, rather than a single total power constraint as in [12] or multiple constraints on the canceller coefficients as in [7]. This approach results in a convex optimization problem which can be solved with the aid of an adequate software package. The associated computational load may be high for systems with a large number of subcarriers, and thus we propose an alternative suboptimal approach with reduced complexity and small performance loss relative to the exact solution.

The paper is organized as follows. Sec. 2 presents the signal model. The spectral peak-constrained AIC designs are presented in Sec. 3. Performance results are given in Sec. 4, and conclusions are drawn in Sec. 5.

2. SIGNAL MODEL AND AIC BASICS

Consider a cognitive OFDM transmitter with N subcarriers. A primary system to be protected from interference is known to operate in frequency band \mathcal{B} within the bandwidth of the cognitive transmitter and spanning N_P contiguous subcarriers. Together with these N_P subcarriers, the AIC scheme allocates N_C more subcarriers for OBR reduction over \mathcal{B} , whereas the remaining $N_D = N - N_P - N_C$ subcarriers are unaffected and used for data transmission.

The $N \times 1$ vector modulating the subcarriers for a given OFDM symbol can be written as $\mathbf{x} = [x_0 \ x_1 \ \dots \ x_{N-1}]^T = \alpha \mathbf{S} \mathbf{d} + \mathbf{T} \mathbf{c}$, where $\mathbf{d} \in \mathbb{C}^{N_D}$ is the zero-mean data vector with covariance $E\{\mathbf{d} \mathbf{d}^H\} = \mathbf{I}_{N_D}$, and $\mathbf{c} \in \mathbb{C}^{N_P+N_C}$ comprises the cancellation coefficients to be modulated on the reserved subcarriers. Matrices $\mathbf{S} \in \mathbb{C}^{N \times N_D}$ and $\mathbf{T} \in \mathbb{C}^{N \times (N_P+N_C)}$ comprise different sets of columns of \mathbf{I}_N , and map the elements of vectors \mathbf{d} and \mathbf{c} , respectively, to their corresponding subcarrier locations. The scaling factor α ($0 < \alpha \leq 1$) controls how the available transmit power is shared between the data and cancellation subcarriers. We take as a baseline the case $\alpha = 1$ and $\mathbf{c} = \mathbf{0}$, i.e., all reserved subcarriers are simply turned off. Hence, $-10 \log_{10} \alpha^2$ denotes the SNR loss (in dB)

incurred by the AIC scheme with respect to the baseline. The OFDM spectrum is the superposition of all subcarrier spectra, affected by their corresponding modulated coefficients x_k :

$$X(f) = \sum_{k=0}^{N-1} x_k \phi_k(f) = \mathbf{x}^T \boldsymbol{\phi}(f), \quad (1)$$

where $\boldsymbol{\phi}(f) \triangleq [\phi_0(f) \ \dots \ \phi_{N-1}(f)]^T$, with $\phi_k(f)$ the *periodic sinc* spectrum¹ of the k -th subcarrier [12, 22].

In general, AIC approaches aim to choosing, for each OFDM symbol, the cancellation vector \mathbf{c} given current data \mathbf{d} , such that the signal spectrum over \mathcal{B} is 'small' in some sense. This symbol-by-symbol optimization, when subject to constraints, may result in high computational load and a difficulty to address spectral peak control. To avoid this complexity issue, we adopt the PSD-based framework from [12], which moves most of the computational load to the offline design of the AIC structure, and results in low implementation (online) cost. Specifically, canceller coefficients are taken as linear combinations of data symbols, i.e., $\mathbf{c} = \boldsymbol{\Theta} \mathbf{d}$, so that

$$\mathbf{x} = (\alpha \mathbf{S} + \mathbf{T} \boldsymbol{\Theta}) \mathbf{d} = \mathbf{G} \mathbf{d}, \quad \text{with } \mathbf{G} \triangleq \alpha \mathbf{S} + \mathbf{T} \boldsymbol{\Theta}, \quad (2)$$

where the weight matrix $\boldsymbol{\Theta} \in \mathbb{C}^{(N_P+N_C) \times N_D}$ is to be optimized. Since $\boldsymbol{\Theta}$ is data-independent, it can be computed offline, and the online complexity of the scheme boils down to the computation of the product $\boldsymbol{\Theta} \mathbf{d}$ for each OFDM symbol.

From (1)-(2), and following [12], the PSD is obtained as

$$P_x(f) \approx E \left\{ |X(f)|^2 \right\} = \text{tr} \{ \mathbf{G}^H \boldsymbol{\Phi}(f) \mathbf{G} \}, \quad (3)$$

with $\boldsymbol{\Phi}(f) \triangleq \boldsymbol{\phi}(f) \boldsymbol{\phi}^H(f)$. Based on (3), the AIC design problem subject to a total power constraint P_{\max} is stated as

$$\min_{\boldsymbol{\Theta}} \int_{\mathcal{B}} P_x(f) df \quad \text{s.t.} \quad \int_{-\infty}^{\infty} P_x(f) df \leq P_{\max}. \quad (4)$$

Introducing the $N \times N$ matrices $\boldsymbol{\Phi}_{\mathcal{B}} \triangleq \int_{\mathcal{B}} \boldsymbol{\Phi}(f) df$ and $\boldsymbol{\Phi}_{\mathcal{T}} \triangleq \int_{-\infty}^{\infty} \boldsymbol{\Phi}(f) df$, (4) can be rewritten as

$$\begin{aligned} \min_{\boldsymbol{\Theta}} \text{tr} \{ \mathbf{G}^H(\boldsymbol{\Theta}) \boldsymbol{\Phi}_{\mathcal{B}} \mathbf{G}(\boldsymbol{\Theta}) \} \\ \text{s.t.} \quad \text{tr} \{ \mathbf{G}^H(\boldsymbol{\Theta}) \boldsymbol{\Phi}_{\mathcal{T}} \mathbf{G}(\boldsymbol{\Theta}) \} \leq P_{\max}, \end{aligned} \quad (5)$$

which is a Least Squares problem with a single quadratic constraint. This problem can be efficiently solved by means of the generalized singular value decomposition [12, 23].

3. SPECTRAL PEAK CONSTRAINED DESIGNS

3.1. Problem formulation and optimal design

While the solution to (5) is optimal in terms of OBR reduction, it is likely to result in unacceptable spectrum overshoot

¹As in [12], conventional cyclic-prefix OFDM is assumed for simplicity.

(see Fig. 1). Hence, our goal is not only to meet the transmit power budget while minimizing OBR, but also to comply with a given spectral mask, keeping spectral spurs below a certain level. To this end, let us denote by \mathcal{D} the frequency band of data subcarriers. We define the peak ratio r as

$$r = \frac{\sup_{f \notin \mathcal{D}} P_x(f)}{\sup_{f \in \mathcal{D}} P_x(f)}. \quad (6)$$

Note that, since $P_x(f)$ depends on Θ , so does r . Using (6), and with r_{\max} a design parameter that controls the admissible level of spectral spurs, our proposed design can be stated as

$$\min_{\Theta} \int_{\mathcal{B}} P_x(f) df \quad \text{s.t.} \quad \begin{cases} r \leq r_{\max} \\ \alpha = 1 \end{cases} \quad (7)$$

Let us focus on the peak constraint $r \leq r_{\max}$ in (7). Let q_0 denote the peak value of the PSD in \mathcal{D} obtained for the baseline scenario ($\alpha = 1$, $\Theta = \mathbf{0}$) in which reserved subcarriers are turned off. Once these cancellation subcarriers are activated according to some AIC design (α , Θ), then if we neglect the effect of these cancellers over \mathcal{D} , we can reasonably approximate $\sup_{f \in \mathcal{D}} P_x(f) \approx \alpha^2 q_0$, which is independent of Θ . On the other hand, as seen in (3), $P_x(f)$ is convex in Θ for every f . Thus, the constraint $r \leq r_{\max}$, which is equivalent to $\sup_{f \notin \mathcal{D}} P_x(f) \leq \alpha^2 q_0 r_{\max}$, is convex [24, Sec. 3.2.3]. Since the objective function is convex, it follows that (7) is a convex problem, for which efficient solvers are available².

Note that in problem (7) the power budget is not taken into account. Nevertheless, its solution, say $\tilde{P}_x(f)$, can be readily scaled to meet the maximum transmit power constraint P_{\max} . Letting $\tilde{P} = \int_{-\infty}^{\infty} \tilde{P}_x(f) df$, and $\bar{\alpha}^2 = P_{\max}/\tilde{P}$, then $\bar{P}_x(f) = \bar{\alpha}^2 \tilde{P}_x(f)$ still satisfies the peak constraint $r \leq r_{\max}$ (since scaling does not change the peak ratio), and its total power is $\int_{-\infty}^{\infty} \bar{P}_x(f) df = P_{\max}$, as desired. The SNR loss incurred is given by $-10 \log_{10} \bar{\alpha}^2$ dB.

3.2. Reduced-Complexity Suboptimal Design

The solution to (7) can be found using an appropriate convex solver. However, this optimal solution may be difficult to compute. For instance, for moderate and large values of N , as in current OFDM standards, the number of entries of Θ to solve for can be very large. In view of this, a reduced-complexity approach is presented next; as will be shown in Sec. 4, its effectiveness is not far from that of the optimal solution, allowing to trade off performance and complexity.

The proposed reduced-complexity design exploits the fact that the solution to problem (4), in which only the total power is constrained, can be obtained efficiently. We notice that the parameter α in (2) is *fixed* when solving (4), and that with smaller values of α more power is allocated to cancellers,

²In practice, the set $f \notin \mathcal{D}$ must be discretized, and the supremum is replaced by the maximum over this discrete set of frequency points; the resulting constraint remains convex [24, Sec. 3.2.3].

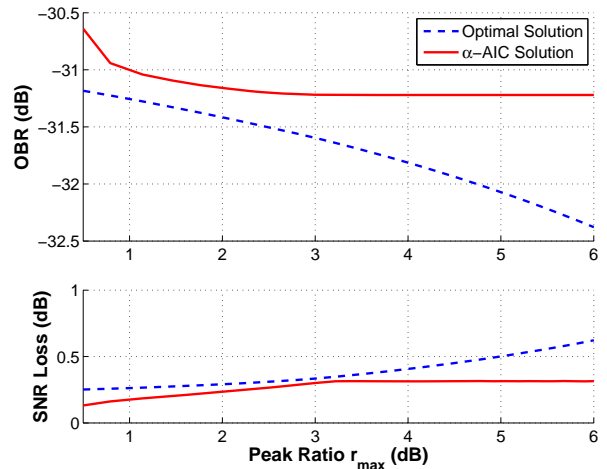


Fig. 2. Performance of the optimal and suboptimal designs. $N = 64$, $N_P = 10$, $N_C = 4$.

with the danger of larger PSD overshoot. Hence, it seems plausible to control spectral spurs by properly tuning α .

We first search for the value α_0 for which the solution of (4) meets $r = r_{\max}$. This value can be easily obtained by means of the bisection method, and determines the range $\alpha_0 \leq \alpha \leq 1$ over which the best power share α_* minimizing OBR and satisfying $r \leq r_{\max}$ is to be searched. To this purpose, we propose a gradient descent search of the form $\alpha_t = \alpha_{t-1} - \delta \nabla(\alpha_{t-1})$, $t = 1, 2, \dots$, where $\delta > 0$ is the stepsize. Note from (2) that the objective function in (5) is quadratic in α for fixed Θ . Neglecting the dependence of Θ with α , we approximate its partial derivative w.r.t. α as

$$\nabla(\alpha_t) \approx \alpha_t \text{tr} \{ \mathbf{S}^T \Phi_{\mathcal{B}} \mathbf{T} \} + \Re \{ \text{tr} [\mathbf{S}^T \Phi_{\mathcal{B}} \mathbf{T} \Theta_t] \}, \quad (8)$$

where Θ_t denotes the solution of (5) at $\alpha = \alpha_t$. The iteration is stopped once $|\alpha_{t+1} - \alpha_t|$ is below some threshold. This suboptimal scheme will be referred to as α -AIC in the sequel.

4. PERFORMANCE EVALUATION

We now evaluate the performance of the novel designs from Sec. 3, and also provide comparisons with the multiple-constraint AIC design (MC-AIC) of [7], and the singular value decomposition-based design (SVD-AIC) from [10]. Both MC-AIC and SVD-AIC are comparable in terms of complexity to the proposed α -AIC design.

We first evaluate the gap incurred by α -AIC w.r.t. the optimal design, i.e. the solution to problem (7) after power normalization. To this end, we consider an OFDM system with $N = 64$ subcarriers and a 5% cyclic prefix. The protected band \mathcal{B} spans $N_P = 10$ subcarriers (indices 20 to 29). A total of $N_C = 4$ cancellation subcarriers is assumed, with indices 18, 19, 30 and 31. In the discretization of the frequency axis, a grid of 5 samples per subcarrier spacing is adopted.

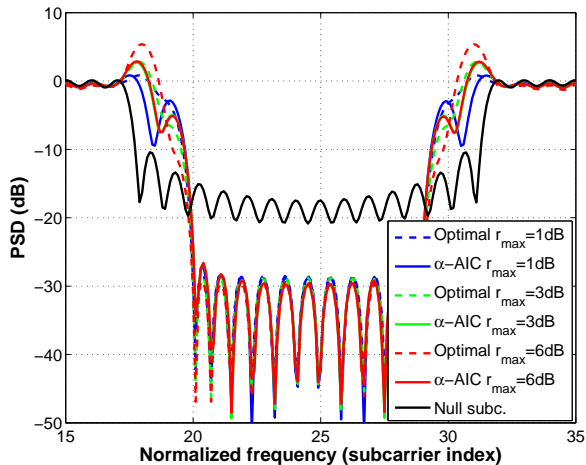


Fig. 3. Power spectra obtained with different designs. $N = 64$, $N_P = 10$, $N_C = 4$.

Fig. 2 shows OBR (expressed in dB relative to the value of the PSD in the subband of data subcarriers) and SNR loss values for the optimal and α -AIC designs, as a function of the maximum peak ratio r_{\max} . As expected, the behavior of both schemes in terms of both OBR and SNR loss is monotone with r_{\max} : as the peak constraint is relaxed, lower OBR levels can be achieved at the expense of a slightly larger SNR loss. It is observed that, when compliance to a tight spectrum mask is required (small r_{\max}), the performance of α -AIC is very close to that of the optimal solution. As r_{\max} is increased, however, a flooring or saturation effect can be observed for α -AIC. This is due to the fact that, for r_{\max} above some value r_* (≈ 3.15 dB in Fig. 2), α -AIC results in a peak ratio $r = r_* < r_{\max}$: the peak constraint is satisfied with strict inequality, and thus further relaxing the constraint does not have an impact on performance. In any case, note that the gap in OBR with respect to the optimal solution remains below 1.5 dB for all $r_{\max} \leq 6$ dB. This is further highlighted in Fig. 3, which shows the PSD of the OFDM signal obtained by both designs and with $r_{\max} = 1, 3$ and 6 dB. In all cases the optimal and α -AIC solutions exhibit significant overlap over \mathcal{B} .

Next we compare the proposed designs against MC-AIC [7] and SVD-AIC [10]. Again, a 5% cyclic prefix is assumed with \mathcal{B} spanning $N_P = 10$ subcarriers, but now we consider $N_C = 8$ cancellation subcarriers (four at each edge of band \mathcal{B}), with different values of the total number of subcarriers ($N = 64, 256$ and 1024). All designs were normalized to have the same total transmit power. For MC-AIC and SVD-AIC, results were obtained by averaging the signal power spectrum over 10^5 OFDM symbols carrying i.i.d. QPSK data. In the case of MC-AIC, all constraints on cancellation subcarriers were set to the same value, and this value was adjusted to obtain the required peak ratio in each case.

Results are shown in Fig. 4. It is noted that SVD-AIC

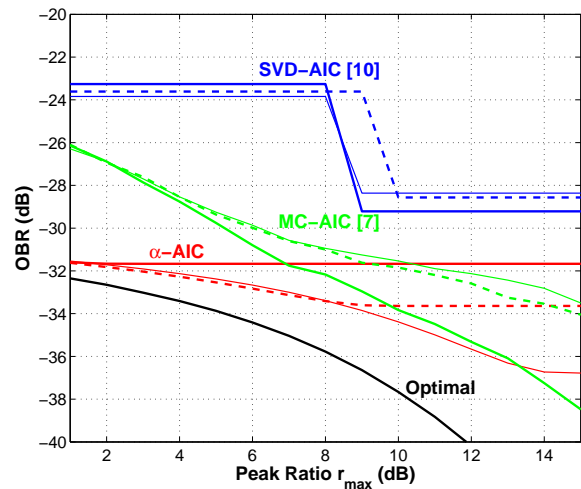


Fig. 4. Performance of α -AIC, MC-AIC and SVD-AIC, for $N = 64$ (solid), $N = 256$ (dashed) and $N = 1024$ (thin solid). Results for the optimal design (7) for $N = 64$ are also shown.

is not flexible enough to provide acceptable results over the range of interest. This is due to the fact that it is not possible to fine-tune the level of the spectral spurs that result as small singular values in the corresponding matrix are discarded. MC-AIC does provide more flexibility in this regard, and for large values of r_{\max} it actually outperforms α -AIC, due to the fact that MC-AIC does not exhibit a flooring effect. Note, however, that the onset r_* of saturation for α -AIC shifts to larger values as N increases. Also, the performance of MC-AIC is seen to degrade with larger values of N , whereas that of α -AIC actually improves. As a result of these facts, α -AIC outperforms MC-AIC in the range of interest (small values of r_{\max}). Note that for $N = 64$, α -AIC is within 1 dB (resp. 3 dB) of the performance of the optimal solution for $r_{\max} \leq 2$ dB (resp. $r_{\max} \leq 6$ dB). The optimal solution for larger N was deemed too costly to compute.

Whereas MC-AIC could in principle yield better results by individually adjusting its constraints on the different cancellers, this is a nontrivial task due to the increased number of degrees of freedom. In contrast, α -AIC is easily tuned for best performance by adjusting a single parameter α .

5. CONCLUSIONS

A novel spectral peak constrained AIC design was presented in order to deal with the spectrum overshoot problem. A formulation in terms of the signal PSD naturally leads to a convex optimization problem. A suboptimal, but more practical, reduced-complexity scheme was proposed with small performance loss for low allowable overshoot levels, as is likely the case in practice. This suboptimal scheme outperforms previous AIC designs of comparable computational cost.

6. REFERENCES

- [1] T. A. Weiss and F. K. Jondral, "Spectrum pooling: an innovative strategy for the enhancement of spectrum efficiency," *IEEE Commun. Mag.*, vol. 42, no. 3, pp. S8–14, Mar. 2004.
- [2] H. Arslan, H. A. Mahmoud, and T. Yucek, "OFDM for cognitive radio: merits and challenges," in *Cognitive Radio, Software Defined Radio, and Adaptive Wireless Systems*, H. Arslan, Ed. Dordrecht, The Netherlands: Springer, 2007.
- [3] H. Yamaguchi, "Active interference cancellation technique for MB-OFDM cognitive radio," in *34th European Microw. Conf.*, vol. 2, Oct. 2004, pp. 1105–08.
- [4] A. Batra, S. Lingam, and J. Balakrishnan, "Multi-band OFDM: a cognitive radio for UWB," in *IEEE Int. Symp. Circuits Syst. (ISCAS)*, May 2006.
- [5] S. Brandes, I. Cosovic, and M. Schnell, "Reduction of out-of-band radiation in OFDM systems by insertion of cancellation carriers," *IEEE Commun. Letters*, vol. 10, no. 6, pp. 420–422, Jun. 2006.
- [6] H. A. Mahmoud and H. Arslan, "Spectrum shaping of OFDM-based cognitive radio signals," in *IEEE Radio and Wireless Symp. (RWS)*, 2008, pp. 113–16.
- [7] S.-G. Huang and C.-H. Hwang, "Improvement of active interference cancellation: avoidance technique for OFDM cognitive radio," *IEEE Trans. Wireless Commun.*, vol. 8, no. 12, pp. 5928–37, Dec. 2009.
- [8] D. Qu, Z. Wang, and T. Jiang, "Extended active interference cancellation for sidelobe suppression in cognitive radio OFDM systems with cyclic prefix," *IEEE Trans. Veh. Technol.*, vol. 59, no. 4, pp. 1689–1695, May 2010.
- [9] E. H. M. Alian, H. E. Saffar, and P. Mitran, "Cross-band interference reduction trade-offs in SISO and MISO OFDM-based cognitive radios," *IEEE Trans. Wireless Commun.*, vol. 11, no. 7, pp. 2436–45, Jul. 2012.
- [10] E. H. M. Alian and P. Mitran, "Improved active interference cancellation for sidelobe suppression in cognitive OFDM systems," in *IEEE Global Commun. Conf. (GLOBECOM)*, Dec. 2012, pp. 1460–65.
- [11] J. F. Schmidt and R. López-Valcarce, "Low complexity primary user protection for cognitive OFDM," in *21st European Signal Process. Conf. (EUSIPCO)*, Sep. 2013.
- [12] J. F. Schmidt, S. Costas-Sanz, and R. López-Valcarce, "Choose your subcarriers wisely: Active interference cancellation for cognitive OFDM," *IEEE J. Emerg. Sel. Topics Circuits Syst.*, vol. 3, no. 4, Dec. 2013.
- [13] I. Cosovic and V. Janardhanam, "Sidelobe suppression in OFDM systems," in *Multi-Carrier Spread-Spectrum*, K. Fazel and S. Kaiser, Eds. Dordrecht, The Netherlands: Springer, 2006.
- [14] S. Pagadarai, R. Rajbanshi, A. Wyglinski, and G. Minden, "Sidelobe suppression for OFDM-based cognitive radios using constellation expansion," in *IEEE Wireless Commun. Netw. Conf. (WCNC)*, 2008, pp. 888–893.
- [15] J. Van De Beek, "Sculpting the multicarrier spectrum: a novel projection precoder," *IEEE Commun. Letters*, vol. 13, no. 12, pp. 881–883, Dec. 2009.
- [16] R. Xu and M. Chen, "A precoding scheme for DFT-based OFDM to suppress sidelobes," *IEEE Commun. Lett.*, vol. 13, no. 10, pp. 776–778, Oct. 2009.
- [17] H.-M. Chen, W.-C. Chen, and C.-D. Chung, "Spectrally precoded OFDM and OFDMA with cyclic prefix and unconstrained guard ratios," *IEEE Trans. Wireless Commun.*, vol. 10, no. 5, pp. 1416–1427, May 2011.
- [18] M. Ma, X. Huang, B. Jiao, and Y. Guo, "Optimal orthogonal precoding for power leakage suppression in DFT-based systems," *IEEE Trans. Commun.*, vol. 59, no. 3, pp. 844–853, Mar. 2011.
- [19] X. Zhou, G. Y. Li, and G. Sun, "Low-complexity spectrum shaping for OFDM-based cognitive radio systems," *IEEE Signal Process. Lett.*, vol. 19, no. 10, pp. 667–670, Oct. 2012.
- [20] J. Zhang, X. Huang, A. Cantoni, and Y. Guo, "Sidelobe suppression with orthogonal projection for multicarrier systems," *IEEE Trans. Commun.*, vol. 60, no. 2, pp. 589–599, Feb. 2012.
- [21] A. Tom, A. Şahin, and H. Arslan, "Mask compliant precoder for OFDM spectrum shaping," *IEEE Commun. Lett.*, vol. 17, no. 3, pp. 447–450, Mar. 2013.
- [22] T. van Waterschoot, V. Le Nir, J. Duplicy, and M. Moonen, "Analytical expressions for the power spectral density of CP-OFDM and ZP-OFDM signals," *IEEE Signal Process. Lett.*, vol. 17, no. 4, pp. 371–374, Apr. 2010.
- [23] G. H. Golub and C. F. Van Loan, *Matrix Computations*, 3rd ed. The Johns Hopkins University Press, Oct. 1996.
- [24] S. Boyd and L. Vandenberghe, *Convex Optimization*. Cambridge University Press, Mar. 2004.